Spatiotemporal Analysis of Urban Nighttime Light After China Lifted 3-Year-Old COVID-19 Restrictions

Ting Hu and Wenqing Shao

***Abstract*—China fully lifted restrictions of the COVID-19 pandemic on December 7, 2022. However, the influence of this policy on urban socioeconomic activities is unclear. Remotely sensed nighttime light (NTL) data have been widely used in evaluating public policies in near real time; therefore, this article attempts to explore the spatiotemporal impact of liberalization on mainland China from the perspective of NTL data. Taking 25 cities with different development levels as representatives, based on daily Black Marble NTL product (VNP46A2), we obtained monthly and weekly averaged NTL images before and after liberalization, and calculated NTL changes in concentric rings to detect the spatiotemporal variations from the urban centers, which can reflect the urban vitality to some degree. Experiment results show that urban NTL radiances within 18 km from urban center are generally on the rise after the lifting of restrictions. The increase of NTL around urban core is the most significant, and the increase intensity decreases exponentially ($R^2 > 0.7$) with the distance from city center or near-center for most cities. Furthermore, NTL radiance generally increases significantly within 1–2 weeks after the lifting in megacities, and different levels of cities responded differently. NTL of megacities and large cities generally changed more rapidly than small–medium cities. Moreover, although mainland China has experienced 3 years of pandemic control, urban development is still underway. The lifting of COVID-19 travel restrictions has brought back the recovery of urban economic vitality. These findings can provide insightful support to urban construction and policy guidance intervention after the pandemic.**

***Index Terms*—Center-periphery structure, nighttime light, spatiotemporal dynamics, the lifting of COVID-19 restrictions, urban vitality.**

I. Introduction

SINCE December 2019, several cases of viral pneumonia have been successively reported in Wuhan, Hubei Province. The World Health Organization said on January 30, 2020 that the pneumonia epidemic caused by the novel coronavirus has constituted a public health emergency of international concern [1]. Since the outbreak of the COVID-19 pandemic, it has caused a huge impact on the natural environment and human society. The pandemic has surged the occurrence of psychological symptoms, such as depression, anxiety, and stress. Besides, it may impair the functioning of human body over time [2]. COVID-19 spread quickly and widely, and hence the number of global infected persons continued to increase. To effectively resist COVID-19, many countries adopted series of nonmedical measures, such as lockdown to slow the rise of the number of infections [3], [4]. However, studies have shown that nonmedical prevention and control measures have an impact on natural environment and social conditions. Prevention and control measures would cause the change natural environment conditions [5]. Also, these measures may affect the temporal choice and spatial characteristics of leisure activities for the youth during the period of lockdown [6]. Different lockdown measures brought different impacts on national gross domestic product (GDP) recovery [7].

During the period of prevention and control, remote sensing technology has played a significant role in monitoring the land surfaces. In order to effectively solve the shortage of medical site, Chinese government utilized remote sensing satellite images to quickly assess the construction environment and conditions, and the construction of Vulcan Mountain Hospital was completed in only 8 days. Meanwhile, as an emerging direction in the field of remote sensing, remotely sensed nighttime light (NTL) is widely used in monitoring of socioeconomic vitality and timely evaluation of public policies by acquiring visible NTL data for area-in-interest [8]. Using DMSP/OLS NTL data from 1992 to 2012, spatiotemporal expansion and driving factors of urban agglomerations were analyzed based on extracting the built-up area in the central plains of China [9]. Besides, many studies have established relationships between NTL radiances and socioeconomic elements, thereby using NTL data to assess the social development [10], [11], [12], [13], [14], [15]. Based on NPP/VIIRS NTL data, a polynomial optimal model was constructed to invert the flood-affected population factor and evaluate the affected area [16]. Shi et al. [17] used Chongqing as study area to analyze poverty based on multisource data, such as NTL and digital elevation model. DMSP/OLS and NPP/VIIRS NTL were used to invert the "urban core-suburban-rural" structure under time-series images [18]. Hu et al. [19] utilized these two kinds

Manuscript received 28 June 2023; revised 6 September 2023 and 21 September 2023; accepted 24 September 2023. Date of publication 27 September 2023; date of current version 5 October 2023. The work was supported in part by the Ministry of Education of Humanities and Social Science Project under Grant 22YJCZH056, in part by the National Natural Science Foundation of China under Grant 42201377, and in part by the Project Supported by the Open Fund of Hubei Luojia Laboratory under Grant 230100025. *(Corresponding author: Wenqing Shao.)*

Ting Hu is with the School of Remote Sensing and Geomatics Engineering, Nanjing University of Information Science and Technology, Nanjing 210044, China, also with the Hubei Luojia Laboratory, Wuhan 430079, China, and also with the Technology Innovation Center for Integration Applications in Remote Sensing and Navigation, Ministry of Natural Resources, Nanjing 210044, China (e-mail: hutingrs@nuist.edu.cn).

Wenqing Shao is with the School of Remote Sensing and Geomatics Engineering, Nanjing University of Information Science and Technology, Nanjing 210044, China (e-mail: swq_0810@163.com).

Digital Object Identifier 10.1109/JSTARS.2023.3319817

of NTL data to model the spatiotemporal dynamics of global electric power consumption for nearly 30 years. Also combined with GDP statistics, NTL was used to analyze spatiotemporal characteristics of economic development in the Yangtze River Delta region [20]. In summary, remotely sensed NTL cannot only promote the integration of NTL with other data, but also promote multidisciplinary development.

Also, NTL data, including DMSP/OLS, NPP/VIIRS and Luojia1-01, have been employed to study the impact of COVID-19 on a wide range of aspects of people's lives, health, and socioeconomic development. Christopher and Daniel [21] utilized NTL to reflect the spatial variation characteristics of the confirmed cases and corresponding impact. Jiang et al. [22] evaluated the changes of socioeconomic factors with the assistance of NTL during the pandemic. Zhang et al. [23] analyzed the heterogeneity of the COVID-19 pandemic on urban economy at different spatiotemporal scales. Yin et al. [24] evaluated the recovery of urban activity in China around the COVID-19 pandemic period in early 2020 by NTL. Lan et al. [25] effectively adopted NTL to assess spatiotemporal changes in human activities induced by COVID-19. Luenam and Puttanapong [26] identified the spatial association between COVID-19 incidence rate and NTL index. Zhao et al. [27] focused on the spatiotemporal changes of NTL along the Sino–Burma border during COVID-19 pandemic. Zhang et al. [28] intended to explore the associations among NTL differences and COVID-19 incidence and mortality in U.S. counties.

In the last 3 years, the Chinese government continuously optimized pandemic prevention and control measures, and fully lifted the 3-year-old restrictions on December 7, 2022 [29]. Previous literature provided information on the urban changes during outbreak prevention and control, and lacked the timely analysis of the impact of the pandemic control liberalization policy. Therefore, this article pays close attention to this policy change in pandemic control, and attempts to investigate the spatiotemporal dynamic of urban NTL after China lifted 3-year-old COVID-19 restrictions. In this article, we selected 25 cities of different spatial distributions and development levels in Chinese mainland territory, and then generated monthly/weekly averaged NTL images based on Black Marble daily NTL product. Concentric ring analysis is commonly employed to explore the spatial pattern of urban elements due to the macroscopically central-peripheral structure of the city [30]. It divides urban areas into a series of rings, which is used to quantify the distance variation of urban elements from city centers [31]; therefore, we employed concentric rings to analyze spatiotemporal dynamics of NTL changes before and after this lifting policy. In addition, we compared NTL images of different years to indirectly reflect the change of urban economic vitality.

The rest of the article is organized as follows. Section II describes datasets and methods we used in this article. Spatiotemporal dynamic of urban NTL changes is presented and reported in Section III. The urban economic vitality recovery in view of NTL is discussed in Section IV. Finally, Section V concludes this article.

II. Datasets and Methodology

A. Datasets

Daily black marble NTL data: We selected NASA's Black Marble VNP46A2 product since it can provide the Earth's NTLs at a daily frequency [32]. Also, compared to its former version (VNP46A1), it has been further refined, such as atmospheric corrected, cloud-removed, and substantial sensitivity enhancement [33]. According to the announcement on the normalization of the pandemic issued by the Chinese government, we downloaded daily NTL images from 1 month (31 days) before the policy to 2 months (62 days) after.

Administrative boundary vector: Related files of the mainland China were obtained from the official website. First, in view of land area and spatial distribution, we chose cities according to geographic location in order to guarantee a balanced distribution. Second, cities are usually of different development levels. We briefly measure the scale of urban development by population size. According to the Chinese Urban Statistical Yearbook and the seventh population census, we divided mainland cities into three levels: megacities, large cities, and small–medium cities. Please mention that Hong Kong, Macao, and Taiwan are not considered in this article.

Baidu Map Pickup Coordinate System (https://api.map.baidu.com/lbsapi/getpoint/index.html) was used to obtain the coordinates of urban centers of selected cities, and the locations were checked and adjusted by referring to Google Maps and Open Street Map. We chose the seat of the municipal people's government as the initial urban center. In order to ensure that the point is in the prosperous area of urban development, Google Maps and Open Street Map were used to check the infrastructure construction and transportation construction around the point. Otherwise, the geographical location of the urban center was finely adjusted. The geographic coordinates of this point can be obtained by Baidu Map Pickup Coordinate System. Finally, nine megacities, eight large cities, and eight small–medium cities, and the coordinates of urban center points are given in Table I.

Urban built-up areas data: Built-up area refers to the land surface that is mainly densely covered by building structures/roads within the administrative area of the city. The built-up area dataset of Chinese cities in 2020 was employed, which is based on the Google Earth Engine cloud platform and generated using Sentinel data [34].

B. Weekly and Monthly Averaged NTL Images

To improve the reliability of NTL data in urban areas, we proposed the following three conditions to remove untrusted pixels. First, the NTL value should fall into valid range, that is, NTL radiance of a pixel is not less than 0 and not equal to 65 535 (the flag of invalid observation). Second, the daily NTL observation should be qualified. Therefore, we used the mandatory flag, quality flag of cloud mask, and snow flag to serve as quality control information. Third, only the NTL observed within the urban built-up area were considered to eliminate the remaining noise.

TABLE I
COORDINATES OF URBAN CENTER POINTS

City level	Representative cities	Urban centers Longitude (° E)	Urban centers Latitude (° N)	Representative cities	Urban centers Longitude (° E)	Urban centers Latitude (° N)
Megacities（9）	Xi'an	108.961	34.272	Shenzhen	114.065	22.549
	Beijing	116.731	39.910	Shanghai	121.480	31.236
	Nanjing	118.766	32.034	Chongqing	106.557	29.570
	Guangzhou	113.271	23.136	Tianjin	117.195	39.086
	Changsha	112.933	28.231			
Large cities（8）	Changchun	125.330	43.823	Taiyuan	112.556	37.877
	Xuzhou	117.278	34.205	Xianyang	108.715	34.336
	Nanchang	115.854	28.687	Yinchuan	106.237	38.494
	Lanzhou	103.832	36.062	Urumqi	87.623	43.832
Small– medium cities（8）	Zhumadian	114.028	33.020	Hengshui	115.675	37.746
	Jingzhou	112.248	30.342	Xinji	115.224	37.950
	Shuozhou	112.427	39.330	Anqing	117.121	30.539
	Zhangjiajie	110.486	29.123	Chenzhou	113.022	25.776

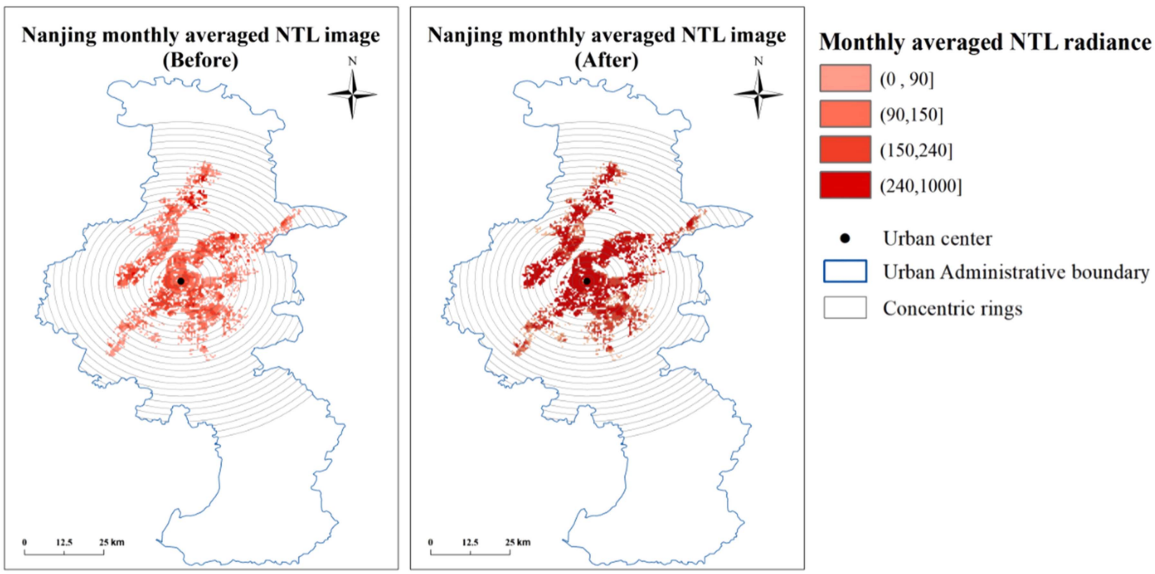

Fig. 1. Monthly averaged NTL images before and after the lifting of restrictions in Nanjing.

Considering the uncertainties of VNP46A2 product and VIIRS instrument [33], we made temporal compositing of VNP46A2 images to generate weekly and monthly averaged NTL data for each city. Taking Nanjing as an example, monthly averaged NTL images before and after this policy are shown in Fig. 1. It can be clearly observed that NTL radiance in Nanjing area increased significantly 1 month after China lifted 3-year-old COVID-19 restrictions.

We further generated a monthly difference image by raster calculation to compare characteristics of spatiotemporal changes of urban NTL. The monthly difference image is defined as follows:

$$\text{Radiance}_{\text{Dif}} = \text{Radiance}_{\text{After}} - \text{Radiance}_{\text{Before}} \quad (1)$$

where $\text{Radiance}_{\text{Dif}}$ refers to the monthly difference NTL radiance value, $\text{Radiance}_{\text{After}}$ is the monthly averaged NTL radiance after the lifting restrictions, and $\text{Radiance}_{\text{Before}}$ is the monthly averaged NTL radiance before China lifted 3-year-old COVID-19 restrictions.

C. Concentric Ring Analysis

Urban center is formed by the concentration of population and socioeconomic elements. Concentric ring division of cities is a commonly used method in the field of urban form and urban disorderly expansion [35]. Concentric ring analysis can well capture the center-periphery structure of a city [36], thereby revealing the variation of urban elements with distance to urban center [37]. It implies the division of urban areas from the center of a city into a series of concentric rings and the dynamic analysis of urban elements under different rings [38].

In this article, two concentric ring division methods were employed for the analysis of monthly and weekly averaged NTL images, respectively, by referring to [39]. The first method was constructing a series of equidistant concentric rings with the interval of 2 km based on the monthly averaged NTL images, to reveal the spatial structure of urban NTL before and after China lifted COVID-19 restrictions. The second one was multidivided concentric rings, spaced at intervals of 3, 5, 10, and 20 km, which were designed for the weekly averaged NTL images, to reflect the change of urban NTL radiance over time. The reason why equidistant concentric ring analysis was not used in temporal analysis will be detailed in Section III-B.

In addition, considering that urban centers may be geographically located near the administrative boundaries of cities, we used the administrative boundary vector to clip the concentric rings, in case that their concentric rings would cover surrounding cities. The above operation ensures that the spatiotemporal dynamics analysis is only focused on the cities of interest. For each concentric ring, we calculated the mean values and standard deviations of NTL radiance changes. The overall workflow of this article is shown in Fig. 2.

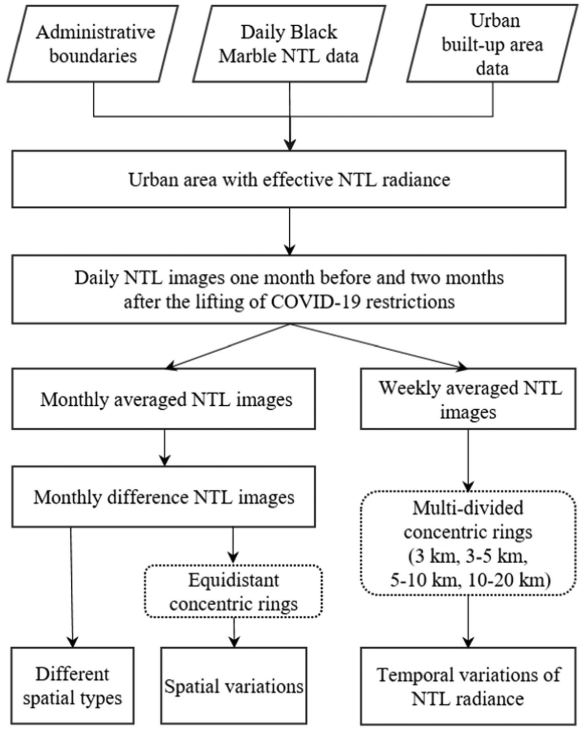

Fig. 2. Overall workflow of this article.

III. Results

A. Different Spatial Types of Urban NTL Changes

We generated the monthly difference NTL image of each selected cities based on the averaged NTL images 1 month before and after China lifted COVID-19 restrictions. For the monthly difference NTL, a negative value indicates a decrease in NTL radiance compared to the NTL value in the period of prevention and control, and a positive value represents an increase in NTL radiance.

Xu et al. [39] defined the uncertain range of VNP46A1 product as $(-20, 20)$ when it was used to analyze NTL changes. In this article, VNP46A2 with higher accuracy was employed. Therefore, the uncertain range should not be larger. We conducted a sensitive analysis to examine the impact of different ranges (i.e., -20 to 20, -10 to 10, and -5 to 5) on the results. It turns out that a wider range like $(-20, 20)$ could ignore some small changes, and the other two ranges lead to broadly consistent results. But the results of $(-10, 10)$ is more robust to data noise. Therefore, we defined difference value ranging from -10 to 10 as the uncertain changes of pixels, and only changes beyond this range were analyzed. The urban NTL changes can be divided into three types, and Fig. 3 shows the spatial distributions for seven representative cities of these three types.

The first kind mainly occurs in large cities and megacities (includes Urumqi, Tianjin, Shenzhen, Taiyuan, and Yinchuan). NTL radiance increases significantly around the area of urban center; however, it decreases in the peripheral area away from the center. The second type is that within the effective urban areas, NTL radiance mainly shows an enhanced spatial distribution. A total of 87.5% of small–medium cities (i.e., Anqing, Hengshui, Jingzhou, Xinji, Zhumadian, Shuozhou, and Chenzhou), 62.5% of large cities (i.e., Xuzhou, Xianyang, Lanzhou, Changchun, and Nanchang), and 77.8% of megacities (i.e., Xi'an, Beijing, Chongqing, Shanghai, Guangzhou, Changsha, and Nanjing) are of the second type. Nearly all the selected cities belong to the former two types, except one small-sized city, Zhangjiajie. There is no significant change in the NTL radiance before and after China lifted 3-year-old COVID-19 restrictions.

B. Spatial Variations of Urban NTL Changes Using Equidistant Rings

We analyzed the monthly difference NTL images by using a series of concentric rings with 2 km interval, and calculated mean values and the standard deviations in different rings of each city. Overall, NTL around urban center changes significantly; however, the change pattern can be divided into the following three types, and the spatial change results of thirteen cities in these three types are shown in Fig. 4. The results of remaining cities are displayed in Figs. 12–13 of the Appendix.

The first type is, as Figs. 4(a) and 12 show, with the increase of distance from city center, the change of NTL radiance gradually rises, reaching the maximum value, and then decreasing to nearly

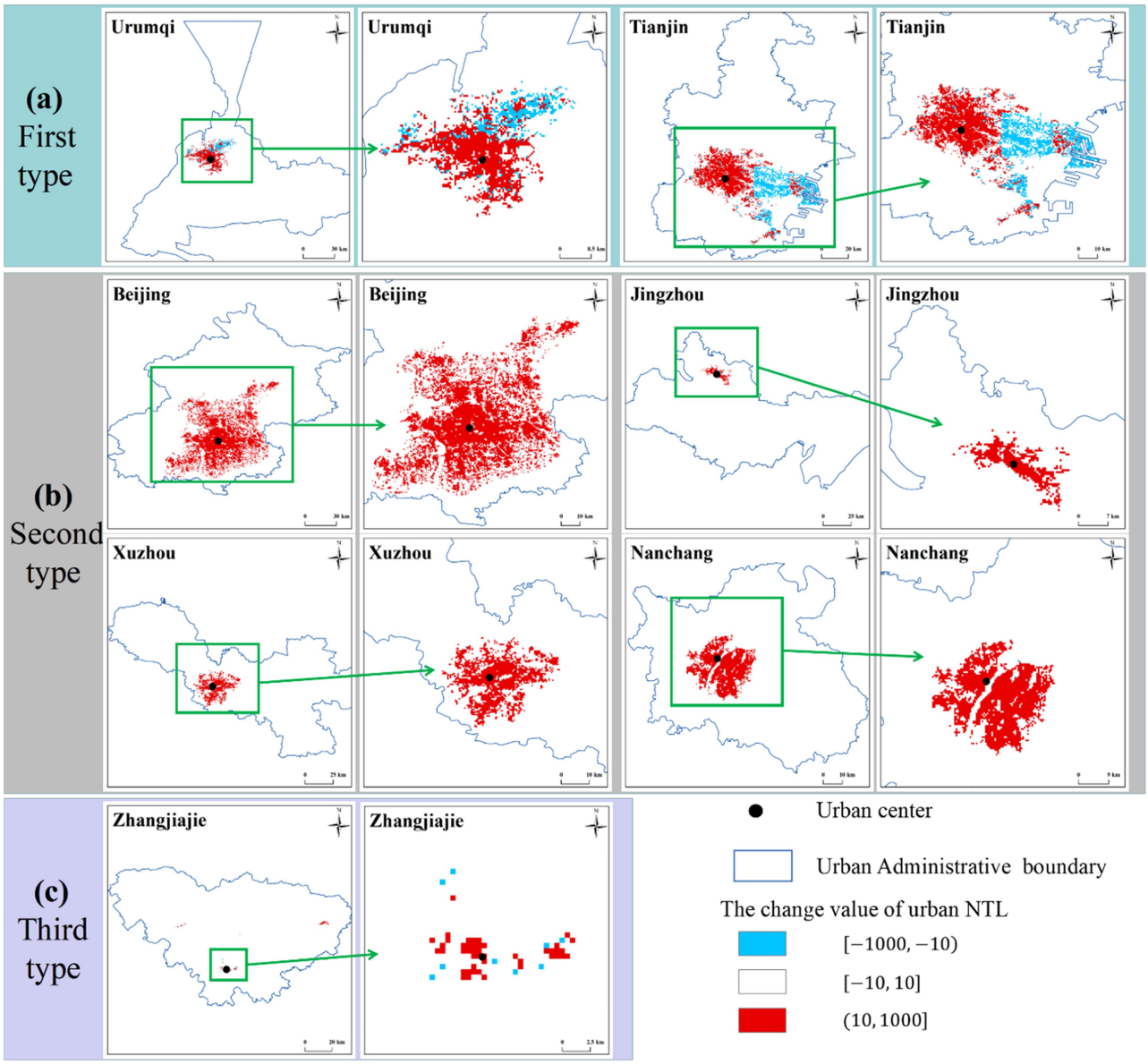

Fig. 3. Different spatial types of urban NTL change value. (a) First type, showing that NTL radiance increases significantly around the area of urban center, however, it decreases in the peripheral area away from the center. (b) Second type, describing that NTL radiance mainly shows an enhanced spatial distribution within the effective urban areas. (c) Third type, showing that there is no significant change in the NTL radiance before and after China lifted 3-year-old COVID-19 restrictions.

zero. We find that all cities in this category have a positive difference value within 18 km from the urban center, indicating that NTL in these areas become brighter after the opening-up. But it increases most significantly at a certain distance from the city center, and then the change of NTL radiance gradually weakens with the distance from the city center. It can be observed that the highest value occurs in the ring about 4–8 km from urban center in these cities. From this ring to more distant one, the changes of NTL gradually weaken. It should be caused by the selection of urban center points. For each city, the urban center point we chose belongs to the prosperous area of the city, but there is a good chance this place would not experience the largest change of light intensity. For example, there were some socioeconomic activities not affected by the pandemic control at the selected center place, which results in the impact of COVID-19 to another prosperous place (only about 4–8 km far from center place) is the most dramatic in the whole city. The first type of trend is mainly found in megacities (i.e., Xi'an, Chongqing, Changsha, and Tianjin) and large cities (i.e., Nanchang, Taiyuan, Yinchuan, Changchun, and Urumqi).

Referring to [30], we applied the inverse-S model in (2) to explore the trend of NTL changes

$$f(r) = \frac{a}{(1 + e^{b-cr})} \tag{2}$$

where f is the value of NTL change, r is the radius from the city center to a concentric ring, e is Euler's number, and a, b, and c are parameters. From Fig. 4(a), we can find that the fitting curves of

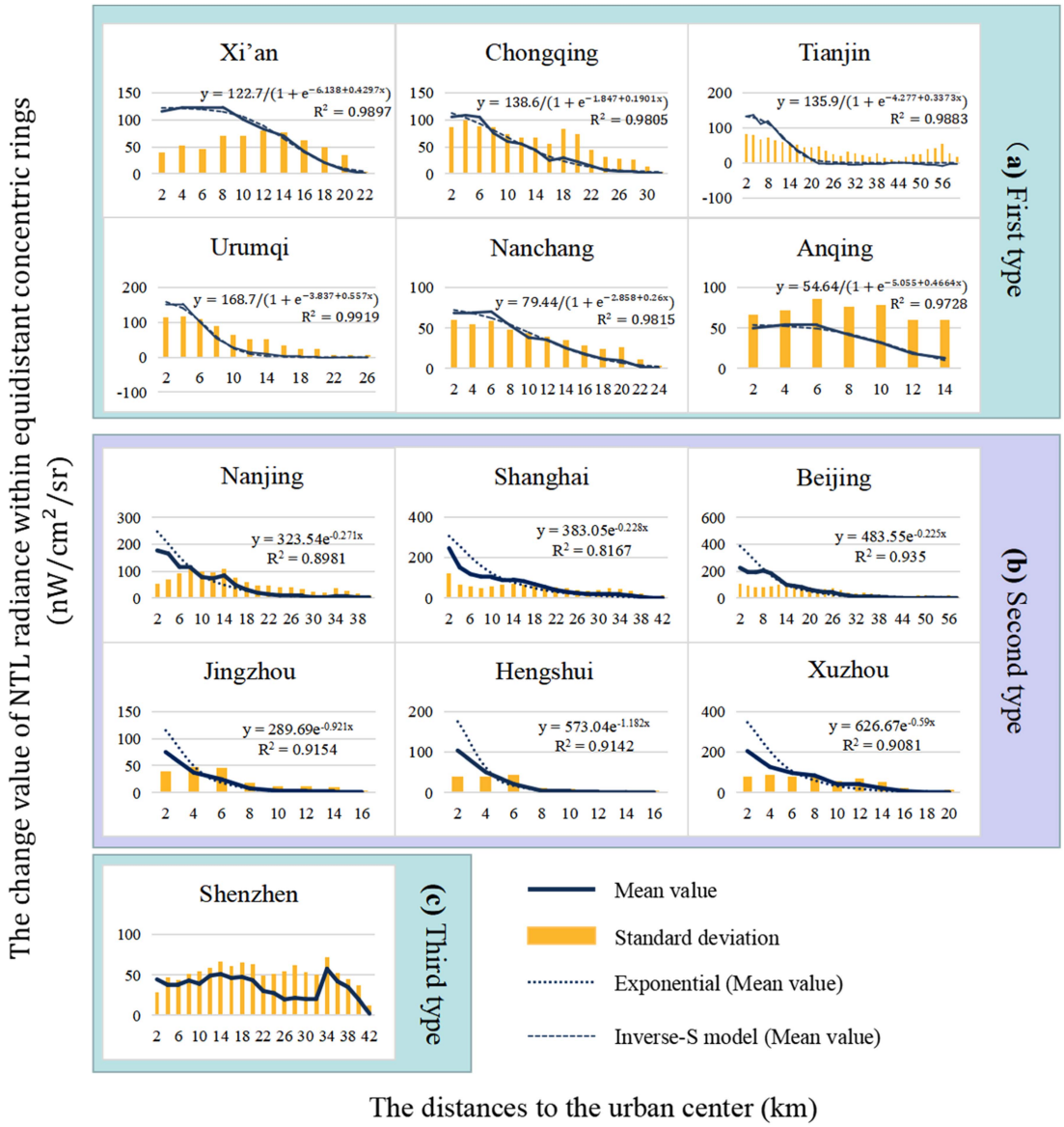

Fig. 4. Spatial variations of urban NTL changes using equidistant rings with 2-km interval. (a) First type is that with the increase of distance from city center, the change of NTL radiance gradually rises, reaching the maximum value, and then decreases to nearly zero. (b) Second type is that the change of NTL radiance shows a tendency of decrease. (c) Third type is that the overall change of NTL radiance exhibits a fluctuating trend.

NTL in these cities are highly in line with inverse-S shape (R^2 above 0.75). For this type, around the central areas, the value of NTL changes remains stable, and then decays quickly, and finally decreases to zero in the outer suburbs.

The second type is shown in Figs. 4(b) and 13, where the change of NTL radiance shows a tendency of decrease. For this type, we employed exponential function to build the relationship. The results show that the change value of urban NTL radiance (y) decreases with the increase of distance (x) from the city center, which is significantly consistent with the exponential model $y = ae^{bx} (a > 0,\ b < 0,\ x > 0)$, with R^2 in all cities not less than 0.7.

Therefore, in this type, the closer to urban center, the more significant the increase in NTL radiance. And the change of NTL radiance decreases exponentially with the increasing distance from city center. A total of 56% of the selected cities (a total of 14 cities) conform to this kind, including 87.5% of small- and medium-sized cities (i.e., Jingzhou, Shuozhou, Chenzhou, Xinji, Hengshui, Zhangjiajie, and Zhumadian), 37.5% of large cities (i.e., Xuzhou, Xianyang, and Lanzhou), and 44.44% of megacities (i.e., Nanjing, Guangzhou, Shanghai, and Beijing).

The third type [Fig. 4(c)] is that the overall change of NTL radiance exhibits a fluctuating trend, and a significant increase at a distance from the city center can be observed. Among all selected cities in this article, Shenzhen belongs to this type. The most significant increase of NTL radiance is found at 34 km from the city center, which is completely different from the above two types.

Considering the influence of urban regional development policies, the internal spatial structure and functional area distribution have evolved from single center to multicenter in several cities,

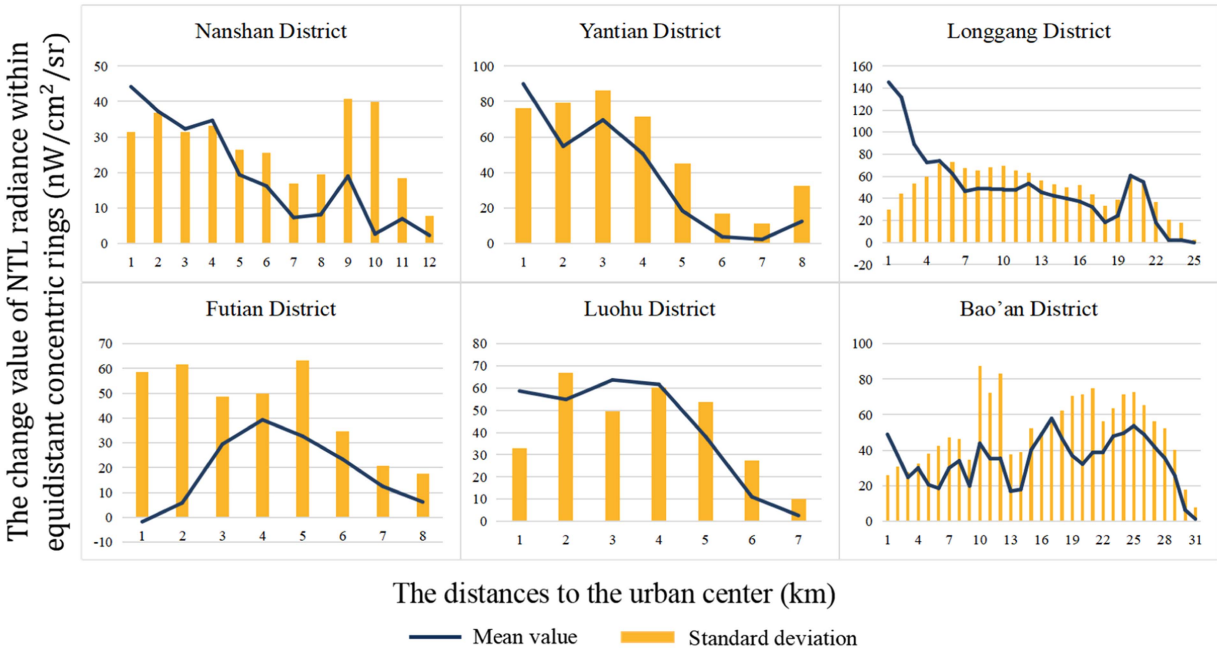

Fig. 5. Spatial variation structure of NTL difference radiance in the administrative districts of Shenzhen using equidistant concentric rings with 1-km interval, including Nanshan district, Yantian district, Longgang district, Futian district, Luohu district, and Bao'an district.

and Shenzhen is basically in line with this trend [40]. Therefore, for the change of NTL radiance in Shenzhen, we made a further analysis from the perspective of a smaller spatial scale, i.e., the district. Shenzhen City is constituted by Luohu District, Futian District, Nanshan District, Bao'an District, Longgang District, and Yantian District.

Specifically, we selected centers of administrative districts to generate a series of concentric rings with 1-km interval for each district, which were used to analyze the monthly difference NTL image. From Fig. 5, we can find that the change of NTL radiance is different in each district. The curves of NTL changes in Yantian, Nanshan, and Longgang Districts all exhibit an attenuation trend (similar to the above mentioned second kind), while the changes of NTL radiance in Futian, Luohu, and Bao'an districts show more similar to the first kind of trend above. Therefore, choosing only one urban center for Shenzhen led to a fluctuate trend of NTL change. It is reasonable to set multicenters in the concentric ring analysis for these polycentric cities, or the changes of NTL radiance would show fluctuations.

In summary, it can be concluded that both exponential model and inverse-S model can describe the spatial variation of NTL changes if center points are selected reasonably. Regardless of the city levels, from central area or near-center to marginal area of the city, the change of urban NTL is getting lower.

C. Temporal Variations of Urban NTL Radiance

To have a knowledge of the impact of opening-up policy on urban NTL changes at a weekly scale, we obtained weekly averaged NTL images of 4 weeks before and 8 weeks after to obtain the NTL changes within different rings (0–3, 3–5, 5–10, and 10–20 km). From the results of spatial patterns in Section III-B, we can observe that the changes of monthly averaged NTL radiances drop significantly with the distance to the city center, which means the NTL changes barely varies in the outer suburbs. If equidistant rings were used for weekly averaged NTL data, the main spatiotemporal patterns could be disturbed by similar but meaningless curves. Therefore, temporal analysis was conducted with nonequidistant rings. Temporal variations of urban NTL radiance of different types of cities are, respectively, displayed in Figs. 6–8, where the abscissa label "−1" represents the first week before the lift of restrictions, and "1" denotes the first week after, and so on. Three main findings can be observed.

First, the timing of significant increase in NTL varies across cities, even for the same city level, indicating the response time to the related policies of each city is different. Taking Nanjing and Tianjin as examples, both cities belong to the megacity type; however, NTL radiance in Nanjing increases significantly in the first week after the release of control, while the rise in Tianjin appears 2 weeks after the opening-up. In addition, after the lifting of restrictions, the NTL in megacities and large cities usually change rapidly, and the response to policies is fast and timely. NTL radiance generally increases significantly within 1–2 weeks after the government lifted COVID-19 restrictions.

Second, the trends of weekly averaged NTL radiance in different rings of the same city are basically consistent in most cases (i.e., Beijing, Nanjing, Taiyuan, and Anqing). Taking Nanjing as an example, weekly averaged NTL radiance in different rings (0–3, 3–5, 5–10, and 10–20 km) is manifested as four different curves, but each polyline has the same inflection position. At the first, fifth, and seventh weeks after the release of control, weekly averaged NTL radiances increase. And at the fourth and sixth weeks after the release of control, weekly averaged NTL radiances decrease. Although the trends in different rings of the

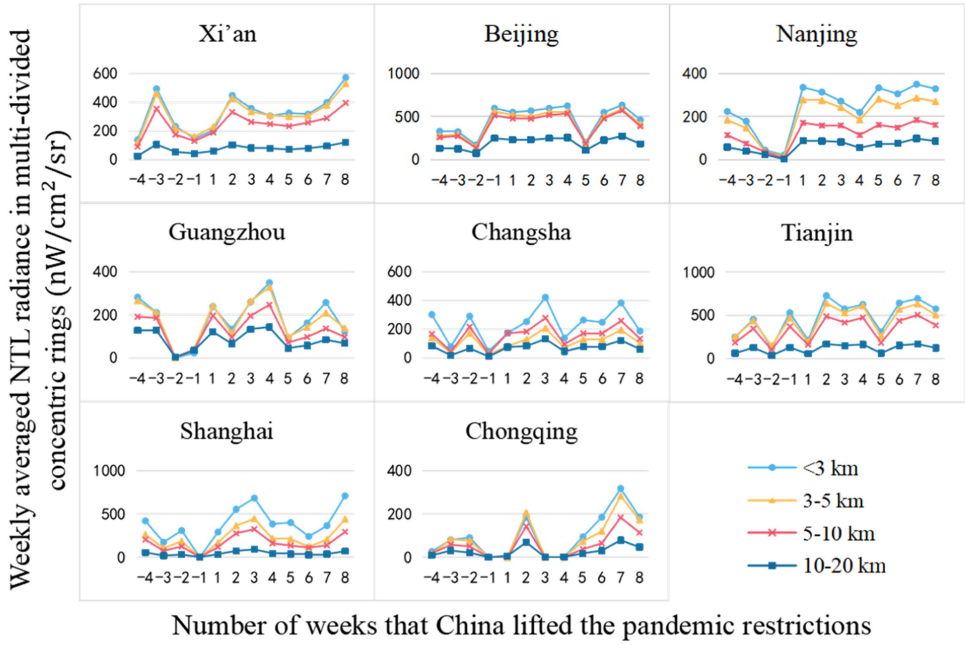

Fig. 6. Temporal variations of weekly averaged NTL radiance using multidivided concentric rings (0–3, 3–5, 5–10, and 10–20 km) in megacities.

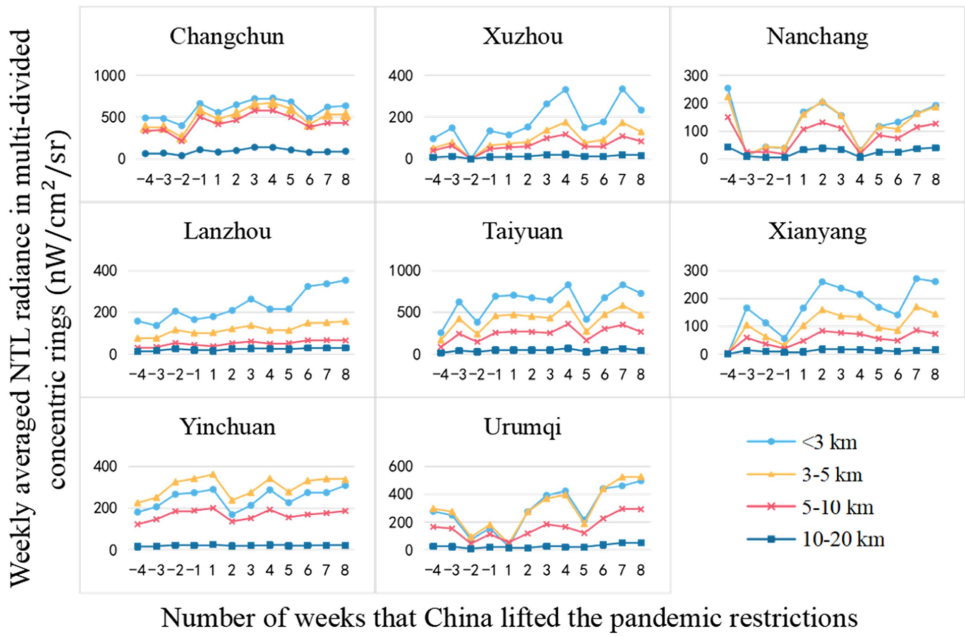

Fig. 7. Temporal variations of weekly averaged NTL radiance using multidivided concentric rings (0–3, 3–5, 5–10, and 10–20 km) in large cities.

same city are basically consistent, the change magnitudes are notably different. For megacities, NTL radiance varies significantly over time within 10 km from urban center; for large and small–medium cities, NTL radiance in the area of 0–5 km away from urban center changes notably in most cases, while NTL radiance in the area of 10–20 km away from urban core only exhibits slight change.

Third, at the fifth to sixth week after the lifting of restrictions, weekly averaged NTL radiance increases significantly in some large cities and small–medium cities (within 5 km from urban center), compared with the previous weeks. Xinhua News Agency said that the annual Spring Festival has officially started on January 13, 2023 [41], and hence Spring Festival travel rush basically started from the fifth week after the lifting of COVID-19 restrictions, i.e., January 8–14, 2023. The large-scale population movement brought by the Spring Festival led to an increase in the weekly averaged NTL radiance in cities with large numbers of migrant

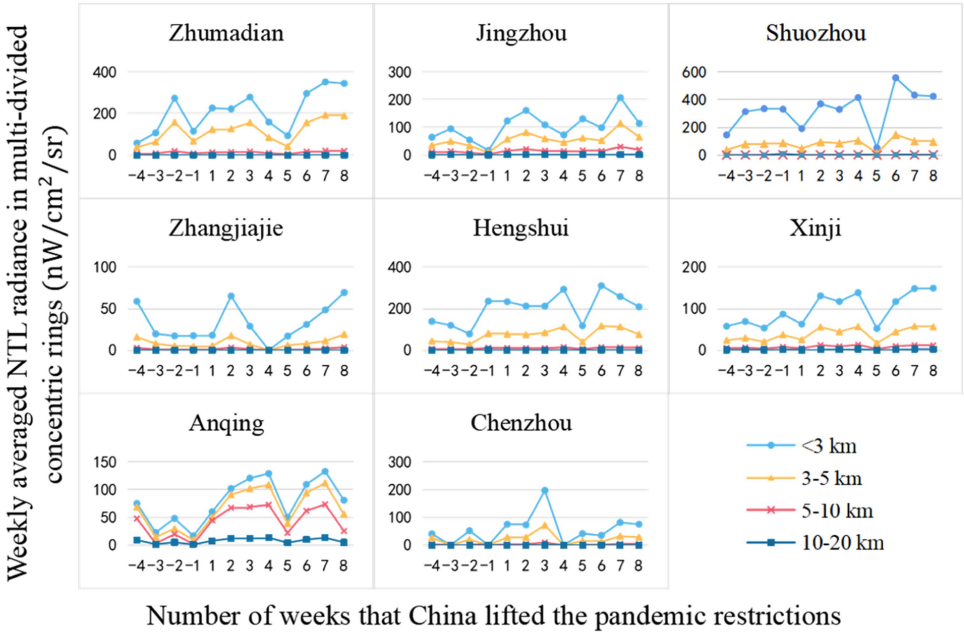

Fig. 8. Temporal variations of weekly averaged NTL radiance using multidivided rings (0–3, 3–5, 5–10, and 10–20 km) in small–medium cities.

workers [42], such as Zhumadian, Anqing, Lanzhou, Urumqi, and Hengshui.

Last but not the least, we focused on the differences in the response of Chinese first-tier cities (i.e., Beijing, Shanghai, and Guangzhou) to the opening-up policy. In Beijing, the NTL radiance began to increase 1 week before the pandemic restrictions were fully lifted. In Shanghai, NTL radiance gradually increased after the lifting of COVID-19 restrictions and reached a maximum in the third week. Guangzhou, as an important central city in China, actively responded to the national policy, and its NTL change was influenced by many factors. Therefore, the NTL radiance of Guangzhou reached a maximum in the first week after the opening up and then fluctuated over time. It can be inferred that as the political center, Beijing could better sense policy changes in advance, while Shanghai took conservative measures to gradually liberalize controls, considering Shanghai has just experienced over 3 months of pandemic prevention and control in the first half of 2022.

IV. Discussions

Urban life generally consists of economic life, social life, and cultural life, and hence urban vitality generally includes three aspects: urban economic vitality, urban social vitality, and urban cultural vitality. It has been widely reported that NTL is correlated with multiple economic indicators, such as GDP and population. Therefore, we believe that NTL data can indirectly reflect the urban vitality, especially the urban economic vitality [43]. In this way, we considered NTL as an indicator of urban vitality. To explore the urban economic vitality recovery, the monthly averaged NTL data before and after the lifting of restrictions were compared and analyzed, according to three city classes: megacities, large cities, and small–medium cities. Considering that at the time we conducted the experiments, the availability of daily Black Marble product was only until March 22, 2023, we utilized the daily NTL dataset from February 20 to March 22 to generate the monthly averaged NTL image after the restrictions was lifted. Therefore, we can exclude the influence of the mass population migration during the Spring Festival. In addition, daily Black Marble images from the same period before the outbreak of COVID-19 (i.e., 2017, 2018, and 2019) were acquired for comparative analysis. Since this time period of 2018 included the Spring Festival, we postponed the start time of the control group to March 1 to obtain the monthly averaged images in 2017–2019. Subsequently, concentric ring analysis was performed to measure the NTL temporal changes in different rings over these years.

Figs. 9–11show the averaged NTL radiances in 2017, 2018, 2019, and 2023 for megacities, large cities, and small–medium cities, respectively. It can be observed that regardless of the city level and ring distance, among 4 years, the NTL intensity in 2023 is higher, and in most cases even the highest. That is, the NTL vibrancy generally returns to the condition of the period when COVID-19 was not outbreak. However, the recovery degree varies from the city level. The NTL radiances of megacities and large cities in 2023 are generally higher than those in other years, while the NTL radiance of small–medium cities are about the same as those in the years before COVID-19.

Furthermore, we selected Changsha, Taiyuan, and Jinzhou as representatives to analyze the NTL radiances of urban core and peripheral areas over these years. In the built-up area of Changsha, the area within 10 km from the city center is defined as urban core, and the area between 22 and 32 km from the city center is regarded as the peripheral area, by referring to [46] and population map of Changsha. In the built-up area of Taiyuan, the area within 6 km from city center is viewed as urban core,

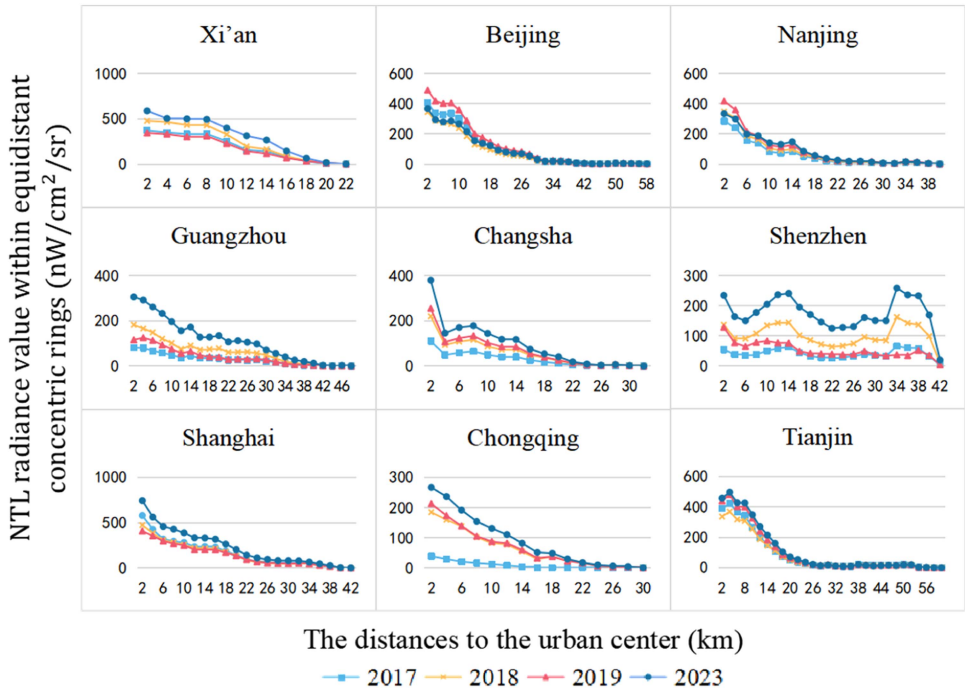

Fig. 9. Monthly averaged NTL radiance value of different years in megacities cities: Xi'an, Beijing, Nanjing, Guangzhou, Changsha, Shenzhen, Shanghai, Chongqing, and Tianjin.

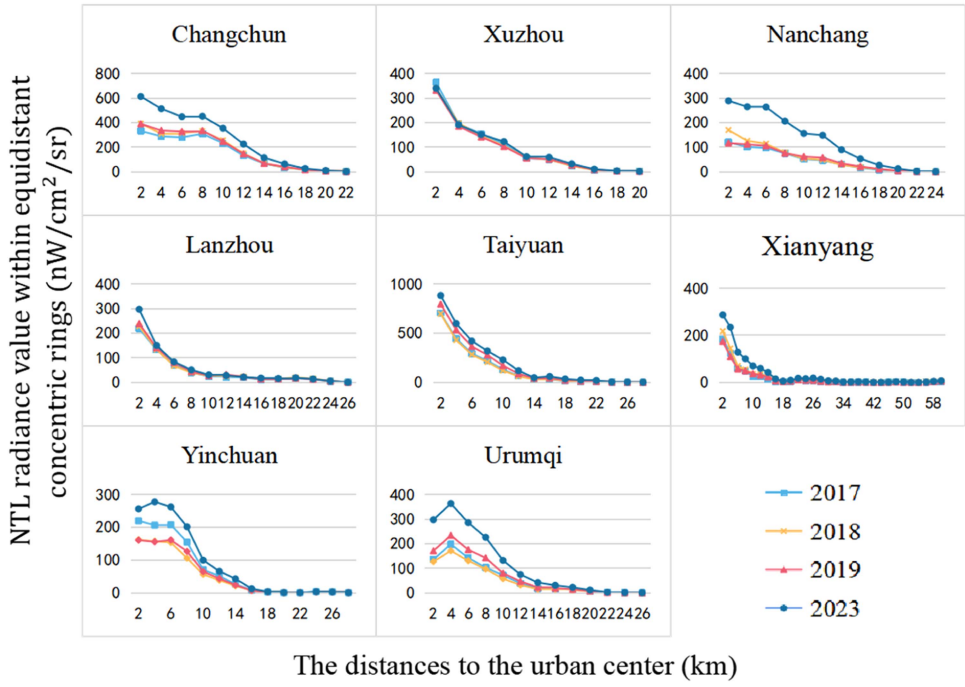

Fig. 10. Monthly averaged NTL radiance value of different years in large cities: Changchun, Xuzhou, Nanchang, Lanzhou, Taiyuan, Xianyang, Yinchuan, and Urumqi.

and the area between 22 and 28 km from city center is defined as the peripheral area. As for Jinzhou, a small–medium city, the thresholds for determining the urban core and peripheral area are 4 and 10–14 km, respectively. The corresponding results of the three cities are listed in Table II, where "Y2023–Y2019" denotes the difference of NTL radiance between year 2023 and 2019. In terms of space, the NTL radiance of all the three cities recovered somewhat after the lifting of restrictions, and the NTL

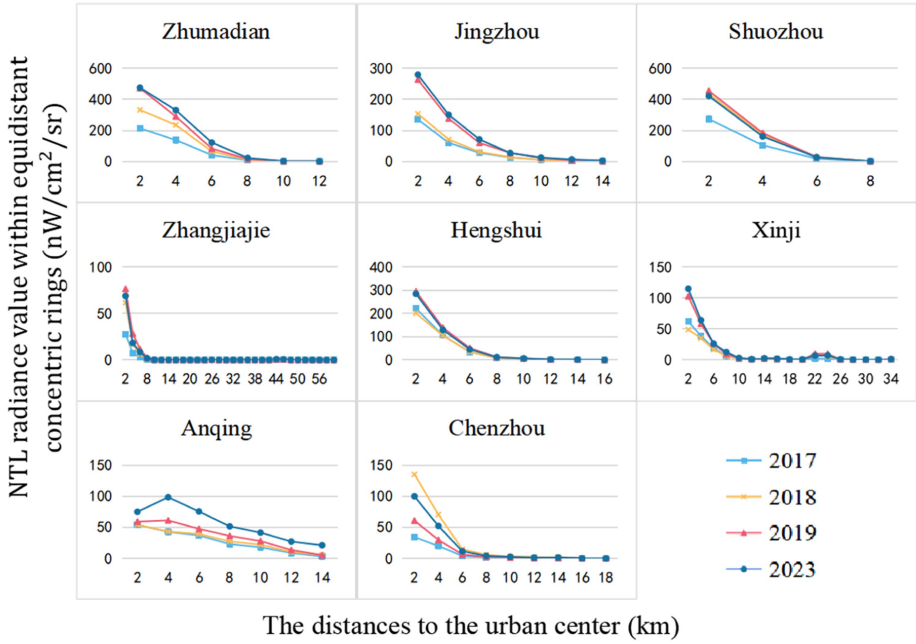

Fig. 11. Monthly averaged NTL radiance value of different years in small–medium cities: Zhumadian, Jingzhou, Shuozhou, Zhangjiajie, Hengshui, Xinji, Anqing, and Chenzhou.

TABLE II
MONTHLY AVERAGED NTL DIFFERENCE IN DIFFERENT AREAS OF CHANGSHA, TAIYUAN, AND JINGZHOU

Area	City	Difference value (nW/cm²/sr)		
		Y2023 – Y2019	Y2023 – Y2018	Y2023 – Y2017
Built-up area	Changsha	61.05	80.19	149.81
	Taiyuan	67.95	143.97	135.55
	Jingzhou	11.08	73.28	81.99
Core area	Changsha	62.17	84.46	150.63
	Taiyuan	62.29	154.43	142.47
	Jingzhou	13.21	91.36	104.06
Peripheral area	Changsha	1.15	1.00	2.85
	Taiyuan	0.99	1.34	1.41
	Jingzhou	2.34	3.42	3.42

recovery intensity of urban core was significantly higher than that of the peripheral area. In terms of time, compared with 2019, the NTL radiance of Changsha and Taiyuan increased significantly after the opening-up policy, and that of Jinzhou only experienced a slight increase. However, the NTL values of all the three cities in 2013 were higher than those in 2017 and 2018.

Therefore, it can be inferred that the lifting of travel restrictions has led to a recovery of urban NTL, and the NTL has returned to levels higher than 2017 and 2018. During the 3-year pandemic period, mainland China still experienced continuous development [47]. The lifting policy promoted the recovery of urban economic vitality and gradually restored normalization of life.

V. CONCLUSION

China has officially fully lifted the travel restrictions of the COVID-19 pandemic on December 7, 2022, which means residents' activities will not be subject to those restrictions induced by the pandemic, such as home quarantine and quarantine for 3 days after arrival at the destination. Therefore, this article investigated the impact of this event on urban residential life and socioeconomic activities from the perspective of NTL remote sensing data.

To have a full understanding of the spatiotemporal dynamics in mainland China, we randomly selected 25 cities with different population sizes and geographical locations as representatives for analysis, including 9 megacities, 8 large cities, and 8 small–medium cities. It can be found that the NTL radiances within the urban centers experienced significant increases in the month following the opening-up event. Basically, the NTL intensity in the first month after opening up is higher than that 1 month before in most cities. In terms of the spatial structure of urban NTL changes, the lift of restrictions brought the most significant increase to the NTL of the central area and the insignificance to the peripheral regions. Both exponential model and the inverse-S function can describe the spatial variation of NTL changes. As for the temporal profile, each city has different response to this lifting policy. Typically, the NTL changed more rapidly in megacities and large cities than in other cities. Finally, we found that compared to the period before pandemic outbreak (2017–2019), urban NTL radiances after the lift of restrictions returned to previous levels in all city ranks, while the recovery degrees varied from different types. Lifting restrictions of COVID-19 has contributed to the recovery of urban economic vitality and mainland China has gradually returned to or even surpassed the socioeconomic level of the nonoutbreak period.

APPENDIX

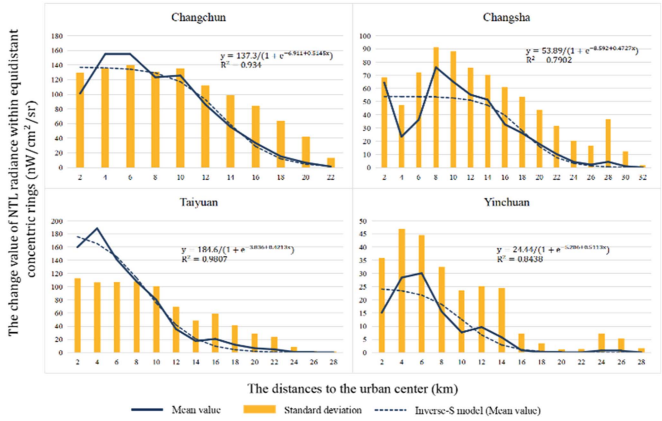

Fig. 12. First type of spatial variation structure in monthly averaged NTL difference images in the remaining cities: Changchun, Changsha, Taiyuan, and Yinchuan.

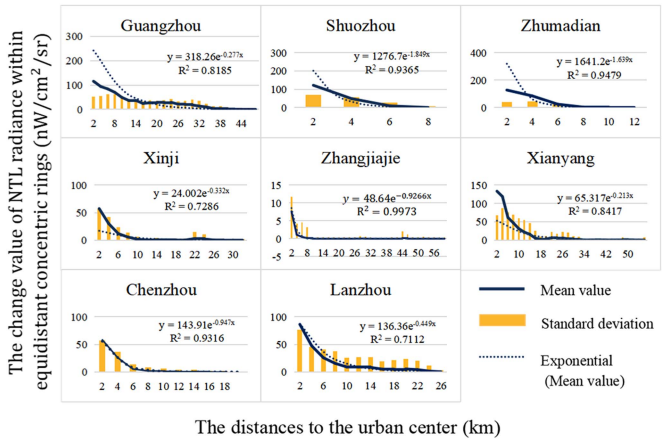

Fig. 13. Second type of spatial variation structure in monthly averaged NTL difference images in the remaining cities: Guangzhou, Shuozhou, Zhumadian, Xinji, Zhangjie, Xianyang, Chenzhou, and Lanzhou.

REFERENCES

[1] "World health organization issues pneumonia outbreak of novel coronavirus infection as a public health emergency of international concern," *China Health Law*, vol. 2, no. 28, 2020, Art. no. 34.

[2] J. Chen, "The impact of the COVID-19 epidemic on mental health and policy implications," *J. Syst. Manage.*, vol. 32, no. 2, pp. 418–427, Mar. 2023, doi: 10.3969/j.issn1005-2542.2023.02.017.

[3] M. U. G. Kraemer et al., "The effect of human mobility and control measures on the COVID-19 epidemic in China," *Science*, vol. 6490, no. 368, pp. 493–497, Mar. 2020, doi: 10.1126/science.abb4218.

[4] S. Lai et al., "Effect of non-pharmaceutical interventions to contain COVID-19 in China," *Nature*, vol. 585, no. 7825, pp. 410–413, May 2020, doi: 10.1038/s41586-020-2293-x.

[5] F. Ramdani and P. Setiani, "Data of satellite observation for environmental assessment before and during COVID-19 pandemic in part of Indonesia using the cloud-computing platform," *Geosci. Data J.*, vol. 9, no. 2, pp. 304–314, Mar. 2022, doi: 10.1002/gdj3.144.

[6] C. Wei, X. Zhu, J. Sun, and Y. Zhang, "Research on the spatial-temporal characteristics and influencing factors of young people's leisure activities in the period of regular epidemic prevention and control: A case study of Nanjing city," *Modern Urban Res.*, vol. 6, pp. 23–30, Jun. 2022, doi: 10.3969/j.issn.1009-6000.2022.06.004.

[7] C. Rattanakul and Y. Lenbury, "Model analysis and simulation on impacts of COVID-19 pandemic on the economy: A case study of Thailand's GDP and its lock down measures," *Int. J. Biol. Biomed. Eng.*, vol. 14, pp. 180–190, Nov. 2020, doi: 10.46300/91011.2020.14.24.

[8] B. Yu et al., "Nighttime light remote sensing and urban studies: Data, methods, applications, and prospects," *Nat. Remote Sens. Bull.*, vol. 25, no. 1, pp. 342–364, Dec. 2021, doi: 10.11834/jrs.20211018.

[9] C. Zhang and L. Hong, "Analysis of spatial and temporal expansion and driving factors of built-up areas in the central plains urban agglomeration based on DMSP/OLS nighttime light data (1992–2012)," *Light Source Lighting*, vol. 63, no. 1, pp. 55–57, Jan. 2022.

[10] Y. Zou, Q. Yan, J. Huang, and F. Li, "Modeling the population density of Su-xi-Chang region based on Luojia-1a nighttime light image," *Resour. Environ. Yangtze Basin*, vol. 29, no. 5, pp. 1086–1094, May 2020, doi: 10.11870/cjlyzyyhj202005004.

[11] L. Cao, P. Li, and L. Zhang, "Urban population estimation based on the DMSP/OLS night-time satellite data—A case of Hubei province," *Remote Sens. Inf.*, vol. 63, no. 1, pp. 83–87, Jan. 2009.

[12] S. Li, L. Li, Q. Xiang, and Z. Ni, "Research of power consumption area estimation and space-time change in Hunan province in recent ten years," *Geomatics Spatial Inf. Technol*, vol. 42, no. 6, pp. 76–80, Jun. 2019.

[13] K. Shi, Y. Chen, L. Li, and C. Huang, "Spatiotemporal variations of urban CO_2 emissions in China: A multiscale perspective," *Appl. Energy*, vol. 211, pp. 218–229, 2018.

[14] M. Zhao, Y. Zhou, X. Li, W. Cheng, and K. Huang, "Mapping urban dynamics (1992–2018) in Southeast Asia using consistent nighttime light data from DMSP and VIIRS," *Remote Sens. Environ.*, vol. 248, Jul. 2020, Art. no. 111980, doi: 10.1016/j.rse.2020.111980.

[15] Q. Zheng, Q. Weng, and K. Wang, "Characterizing urban land changes of 30 global megacities using nighttime light time series stacks," *ISPRS J. Photogrammetry Remote Sens.*, vol. 173, pp. 10–23, Jan. 2021, doi: 10.1016/j.isprsjprs.2021.01.002.

[16] Y. He, X. Wang, C. Cai, D. Cai, Y. Zheng, and D. Li, "Flood damage assessment and visualization based on NPP-VIIRS nighttime light remote sensing," *J. Natural Disasters*, vol. 31, no. 3, pp. 93–105, Jun. 2022, doi: 10.13577/j.jnd.2022.0309.

[17] K. Shi, Z. Chang, Z. Chen, J. Wu, and B. Yu, "Identifying and evaluating poverty using multisource remote sensing and point of interest (POI) data: A case study of Chongqing, China," *J. Cleaner Prod.*, vol. 255, 2020, Art. no. 120245, doi: 10.1016/j.jclepro.2020.120245.

[18] Y. Huang, J. Yang, M. Chen, C. Wu, H. Ren, and Y. Liu, "An approach for retrieving consistent time series 'urban core–suburban-rural' (USR) structure using nighttime light data from DMSP/OLS and NPP/VIIRS," *Remote Sens.*, vol. 14, no. 15, Jul. 2022, Art. no. 3642, doi: 10.3390/rs14153642.

[19] T. Hu, T. Wang, Q. Yan, T. Chen, S. Jin, and J. Hu, "Modeling the spatiotemporal dynamics of global electric power consumption (1992–2019) by utilizing consistent nighttime light data from DMSP-OLS and NPP-VIIRS," *Appl. Energy*, vol. 322, Jun. 2022, Art. no. 119473, doi: 10.1016/j.apenergy.2022.119473.

[20] M. Yan, "Spatial analysis of GDP in the Yangtze river delta region based on night light data," M.S. thesis, Dept. School Geogr. Sci., Liao Ning Normal Univ., Liao Ning, China, 2022.

[21] S. Christopher and S. Daniel, "Spatiotemporal evolution of COVID - 19 infection and detection within night light networks: Comparative analysis of USA and China," *Appl. Netw. Sci.*, vol. 1, no. 6, 2021, Art. no. 10.

[22] Z. Jiang, J. Deng, H. Luan, and L. Li, "Rapid extraction of COVID-19 information based on nighttime light remote sensing: A case study of Beijing," *Bull. Surveying Mapping*, vol. 7, pp. 43–48, 2022, doi: 10.13474/j.cnki.11-2246.2022.0201.

[23] X. Zhang, H. Wang, X. Ning, and R. Liu, "Spatio-temporal difference analysis of the economic impact of the COVID-19 outbreak on urban economy," *Sci. Surveying Mapping*, vol. 47, no. 4, pp. 189–198, Apr. 2022.

[24] R. Yin et al., "Night-time light imagery reveals China's city activity during the COVID-19 pandemic period in early 2020," *IEEE J. Sel. Topics Appl. Earth Observ. Remote Sens.*, vol. 14, pp. 5111–5122, 2021, doi: 10.1109/JSTARS.2021.3078237.

[25] T. Lan, G. Shao, L. Tang, Z. Xu, W. Zhu, and L. Liu, "Quantifying spatiotemporal changes in human activities induced by COVID-19 pandemic using daily nighttime light data," *IEEE J. Sel. Topics Appl. Earth Observ. Remote Sens.*, vol. 14, pp. 2740–2753, 2021, doi: 10.1109/JSTARS.2021.3060038.

[26] A. Luenam and N. Puttanapong, "Spatial association between COVID-19 incidence rate and nighttime light index," *Geospatial Health*, vol. 17, no. s1, Feb. 2022, Art. no. 35735945, doi: 10.4081/gh.2022.1066.

[27] F. Zhao, S. Zhang, and D. Zhang., "Illuminated border: Spatiotemporal analysis of COVID-19 pressure in the Sino–Burma border from the perspective of nighttime light," *Int. J. Appl. Earth Observ. Geoinf.*, vol. 109, Apr. 2022, Art. no. 102774, doi: 10.1016/j.jag.2022.102774.

[28] Y. Zhang, N. Peng, S. Yang, and P. Jia, "Associations between nighttime light and COVID-19 incidence and mortality in the United States," *Int. J. Appl. Earth Observ. Geoinf.*, vol. 112, Jun. 2022, Art. no. 102855, doi: 10.1016/j.jag.2022.102855.

[29] "Notice on further optimization of the implementation of measures for the prevention and control of COVID-19," Chinese Center for Disease Prevention, China, 2022. Accessed: Dec. 7, 2022. [Online]. Available: https://www.chinacdc.cn/jkzt/crb/zl/szkb_11803/jszl_11815/202212/t20221207_262957.html

[30] M. Zheng, W. Huang, G. Xu, X. Li, and L. Jiao, "Spatial gradients of urban land density and nighttime light intensity in 30 global megacities," *Humanities Social Sci. Commun.*, vol. 10, 2023, Art. no. 404, doi: 10.1057/s41599-023-01884-8.

[31] S. Wu, N. S. Sumari, T. Dong, G. Xu, and Y. Liu, "Characterizing urban expansion combining concentric-ring and grid-based analysis for Latin American cities," *Land*, vol. 10, no. 5, 2021, Art. no. 444, doi: 10.3390/land10050444.

[32] M. O. Román et al., "NASA's black marble nighttime lights product suite," *Remote Sens. Environ.*, vol. 210, pp. 113–143, Mar. 2018, doi: 10.1016/j.rse.2018.03.017.

[33] Q. Zheng, Q. Weng, Y. Zhou, and B. Dong, "Impact of temporal compositing on nighttime light data and its applications," *Remote Sens. Environ.*, vol. 274, Mar. 2022, Art. no. 113016, doi: 10.1016/j.rse.2022.113016.

[34] J. Sun et al., "A dataset of built-up areas of Chinese cities in 2020," *China Sci. Data*, vol. 7, no. 1, pp. 184–198, Mar. 2022, doi: 10.11922/11-6035.csd.2021.0087.zh.

[35] L. Jiao, "Urban land density function: A new method to characterize urban expansion," *Landscape Urban Plan.*, vol. 139, pp. 26–39, 2015, doi: 10.1016/j.landurbplan.2015.02.017.

[36] M. Guérois and D. Pumain, "Built-up encroachment and the urban field: A comparison of forty European cities," *Environ. Plan. A*, vol. 40, no. 9, pp. 2186–2203, 2008, doi: 10.1068/a39382.

[37] L. Jiao, T. Dong, G. Xu, Z. Zhou, J. Liu, and Y. Liu, "Geographic micro-process model: Understanding global urban expansion from a process-oriented view," *Comput. Environ. Urban Syst.*, vol. 87, Feb. 2021, Art. no. 101603, doi: 10.1016/j.compenvurbsys.2021.101603.

[38] S. Wu, N. S. Sumari, T. Dong, G. Xu, and Y. Liu., "Characterizing urban expansion combining concentric-ring and grid-based analysis for Latin American cities," *Land*, vol. 10, no. 5, Apr. 2021, Art. no. 444, doi: 10.3390/land10050444.

[39] G. Xu, T. Xiu, X. Li, X. Liang, and L. Jiao, "Lockdown induced nighttime light dynamics during the COVID-19 epidemic in global megacities," *Int. J. Appl. Earth Observ. Geoinf.*, vol. 102, Jun. 2021, Art. no. 102421, doi: 10.1016/j.jag.2021.102421.

[40] H. Zhang, "A study of intra-city polycentricity in the post-industrial era: A case of Shenzhen," M.S. thesis, School Econ., Jinan Univ., Guangzhou, China, 2015.

[41] H. Ye, X. Fan, Y. Zhou, and X. Li, *2023 Spring Festival meets Big Test*. Beijing, China: Xinhua Daily Telegraph, 2023.

[42] Z. Zhao, Y. Wei, R. Pang, R. Yang, and S. Wang, "Spatiotemporal and structural characteristics of interprovincial population flow during the 2015 spring festival travel rush," *Prog. Geogr.*, vol. 36, no. 8, pp. 952–964, Aug. 2017, doi: 10.18306/dlkxjz.2017.08.004.

[43] W. Liu et al., "Dynamic monitoring of recovery after the 2017 Jiuzhaigou earthquake based on NPP-VIIRS night light data," *Beijing Surveying Mapping*, vol. 36, no. 12, pp. 1738–1745, Dec. 2022, doi: 10.19580/j.cnki.1007-3000.2022.12.023.

[44] Y. Zhou, X. He, and B. Zikirya, "Boba shop, coffee shop, and urban vitality and development-a spatial association and temporal analysis of major cities in China from the standpoint of nighttime light," *Remote Sens.*, vol. 15, 2023, Art. no. 903, doi: 10.3390/rs15040903.

[45] G. Xu, J. Su, C. Xia, X. Li, and R. Xiao, "Spatial mismatches between nighttime light intensity and building morphology in Shanghai, China," *Sustain. Cities Soc.*, vol. 81, 2022, Art. no. 103851.

[46] H. Lu, Z. Bai, Z. Wu, and Z. Fu, "Reasonable scale of megacity central area based on multivariate data and a traffic perspective," *Strategic Study CAE*, vol. 24, no. 6, pp. 146–153, 2022, doi: 10.15302/J-SSCAE-2022.06.013.

[47] H. Xu and S. Hu, "Development disparity of major urban agglomerations in Yangtze river economic zone under perspective of night-time light," *Resour. Environ. Yangtze Basin*, vol. 32, no. 1, pp. 14–23, Jan. 2023, doi: 10.11870/cjlyzyyhj202301002.

Ting Hu received the master's degree in photogrammetry and remote sensing from the Wuhan University, Wuhan, China, in 2015, and the Ph.D. degree in photogrammetry and remote sensing from the Wuhan University, Wuhan, China, in 2020.

She is currently an Associate Professor with the School of Remote Sensing and Geomatics Engineering, Nanjing University of Information Science and Technology, Nanjing, China. Her research interests include remote sensing image analysis and remote sensing applications.

Wenqing Shao received the B.Eng. degree in remote sensing science and technology from the School of Remote Sensing & Geomatics Engineering, Nanjing University of Information Science & Technology, Nanjing, China, in 2023. She is currently working toward the M.S. degree in cartography and geography information system with the School of Geography, Nanjing Normal University, Nanjing, China.

Her research interests include remote sensing mapping and cartographic visualization.